

Design and Analysis of a 5-Axis Gantry CNC Machine Tool

Esra Yuksel¹, Emre Özlü^{1}, Ahmet Oral², Fulya Tosun², Osman Fatih İğrek², Erhan Budak¹*

¹Manufacturing Research Lab, Sabanci University, Tuzla, İstanbul, Turkey

²İğrek Makina Döküm Inc.,OSB A.O. Sönmez Bulv. No:10 16140 Bursa, Turkey

Abstract. In this study, the design and analysis of a gantry-type 5-axis CNC machine tool are presented with experimental results on a manufactured prototype. Critical points in the design of a large-scale and heavy-duty machine tool are discussed. Moreover, FE analysis results are also presented with detailed discussion. The measurement results on structural dynamics are shown together with the FE results. Furthermore, the final performance of the machine tool is demonstrated thorough the position and velocity measurements of the axes.

1 Introduction

The fast and competitive development of aerospace, automotive, and die/mold industries drive machine tool companies to offer better solutions for heavy-duty machining applications. Gantry-type machine tools are one of the most suitable structures with expandable machining spans, significant structural rigidity properties, reliable promises for motion precision, and accuracy [1]. A competitive heavy-duty 5-axis gantry milling machine can process workpieces that are ranged from 16 to 20 tones, with 8 to 10 μm axial precision at X and Y of machine coordinates, while positional accuracy ranges from 10 to 15 μm for these axes. Generally, forkhead spindle structures are employed for heavy-duty 5-axis gantry-type milling machines with 95 to 120 degrees rotation capacity at A-axis, while C-axis can rotate 360 degrees. Speed of forkhead spindles, that are mounted on gantry-type 5-axis CNCs, range from 5000 to 25000 rpm for heavy-duty machining applications. Axial and positional accuracy/precision of the Z column can change between 3 and 5 μm . In this study, the subjected 5-axis milling machine has an X-axis (gantry) with a length of 6700 mm. Similarly, Y-axis has a length of 3500 mm. These dimensions are longer than the usual standards. Thus, there must be three main considerations as well as the other considerations mentioned in [2] to produce such a massive machine tool: i) production technique of the machine tool components and material selection, ii) structural reliability and stiffness, iii) thermal behaviour, and robustness.

Generally, welded or casted components are employed for the construction of gantry-type milling machines that are employed for heavy-duty machining applications. The usage of welded components and joints-especially during the construction of a machine base and

* Corresponding author : emre.ozlu@sabanciuniv.edu

mainframes- is an emerging trend due to lower manufacturing costs compared to casted complex machine tool parts [3,4]. Moreover, welding techniques allow usage of carbon-fiber based composites in machine tool structures which can be structurally reliable as casted components [5,6]. However, the anisotropic properties of these composites cannot maintain the required stiffness levels for long structural components and spindle structures of machine tools [5]. Besides, Gas Metal Arc Welding (GMAW), Manual Metal Arc Welding (MMAW) and Laser Arc-Hybrid Welding (LAHW) are employed for welding of thick metal components [7], and welded materials with these techniques reach their melting points which can cause distortion, porosity, and weak material properties [8]. As a result, Y-axis strokes between 2500 and 3000mm are accepted as standard lengths for large-scale 5-axis gantry-type machine tools that are produced with welding techniques. Thus, to be able to extend the stroke of X and Y axes, casted components with superior damping properties are required to maintain the desired stiffness properties [9]. Another way to forecast and maintain the required stiffness values is to employ FEM and structural optimization techniques [10], such as topology, shape, or crossbeam optimizations [1,10,11]. During the structural design and optimization of a large-scale gantry-type machine tool, major parameters are as follows: i) The structural properties of the gantry are important since this component generally assembles with welding joints which can cause loss of stiffness. Therefore, the research in the literature focuses on crossbeam optimization for gantry components to improve the stiffness behaviour on heavy-duty machine tool structures. [1,10]. ii) Modeling of mechanical interfaces in FE analyses is critical during the simulation and structural optimization for even regular-size machine tools [13], thus, massive component sizes and weights make contacts more critical for large-scale machine tools. iii.) Moreover, thermal compensation techniques are not very effective for large-scale machine tools. Additionally, thermal design/optimization requires advanced techniques for thermal distortion detection and compensation even for a medium gantry-type 5-axis CNC machine [10]. Therefore, designs for preventing thermal distortions are more effective in large-scale machine tools.

Regarding the facts mentioned above, this study proposes casting method-benefited design strategies for a 5-axis gantry-type CNC machine tool. The effectiveness of the proposed strategies is evaluated with FE analyses and experiments on a prototype machine tool manufactured.

2 Design of the Machine Tool and Control System

The proposed casting-method benefited design strategies are as follows: The mainframes are designed as casted mono-block parts, which makes this design unique compared to other CNC structures in the machine tool industry. The mono-block main bodies will imitate a single-volume structure when geometric and dynamic behaviour are considered. The superiority of the casted materials over the welded ones is their damping ability. Especially, the damping ability of Gray iron is at least threefold of steel structures [14]. Frames of X and Y axes and machine bases are made of GG25, and GG50 is employed to build Z-axis. The base part of the milling machine is also cast as a mono-bloc piece which weighs 24 tons. Therefore, the first mode of the structure is expected to demonstrate a mode shape of a single-volume structure. The X-axis of the machine (gantry) is longer than the usual standards. Thus, the usage of casted components may not enough to maintain the required stiffness. Therefore, the internal structure of the gantry is supported by special ribbing elements. Additionally, pretensions are directed to the gantry surface during the casting process. Moreover, rails of the linear guides are cast with these mono-block components to avoid structural deformations on X and Y axes of the machine. The pretensions and casted railways are indicated in Fig.1. b. Additionally, a rack and pinion

system based linear motion mechanism is employed instead of classic drive screw systems. This type of linear motion mechanism exposes lesser efficiency losses. Moreover, the structural configuration of the rack and pinion system on the gantry provides additional support for the Z column as shown in Fig.1. a. As mentioned earlier, designs for preventing thermal distortions are more effective compared to thermal compensation techniques during the design stage of large-scale machine tools. Thus, as a cooling precaution, pipelines are inserted under the slideways of X and Y axes for water circulation to keep the temperature change in the minimum. These pipes are inserted during the casting process. The pipeline locations for mainframe cooling can be seen on the manufactured prototype in Fig.1. c.

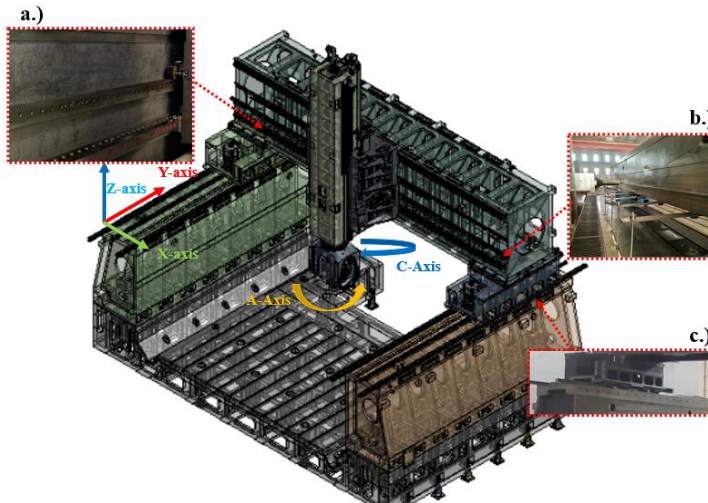


Fig.1: CAD data of the 5-axis CNC with general machine coordinates, a.) The rack and pinion system used for linear motion system, b.) The pretensions on the gantry surface due to casting, and casted rails of linear guideways, c.) The pipeline locations for the cooling of mainframes.

3 FE Analyses

The CAD model of the assembly was simplified, and the simplified version of the CAD model was composed of 377 parts in total. 14,117,354 pyramid mesh elements were employed with 2,538,140 nodes after Jacobian and skew ratio checks. The pure penalty algorithm (prone to assign higher and oscillative contact stiffness values [13]) was employed with 0.2 % relaxation tolerance on the contact interfaces.

3.1 Static Analysis

The gravitational force was applied at the - Z-axis direction of the machine tool coordinates. The structure was fixed from the pads under the machine base. The FE model was positioned at the least stiff position to be able to detect the maximum deflection amount. The total deflection of the CNC structure is shown in Fig.2i.a. which is 0.164 mm. Fig.2i.a. indicates that spindle-gantry connection is the weakest point of the structure. However, the total deformation of the gantry is predicted as 0.109 mm while these deformations are detected as 0.002mm for X-axis. 0.03 mm and 0.09mm deflection are obtained for Y and Z axes, respectively. These results can be interpreted as the rigidity effect of the casted mono-block base and mainframes on the gantry. The directional

deformations are illustrated in Fig.2. b., c., and d. The maximum deformation is found as 0.002 mm on the X-axis, and it proves that the mono-block cast frames behave like a single volume. 0.07 mm and 0.149 mm deflection are detected on the Y and Z axes, respectively.

3.2 Dynamic Analysis

Subsequently, modal analysis was employed to find the natural frequencies of the structure. The results indicate a natural frequency range between 20 and 70 Hz, which is smaller compared to regular-size machine tools. It is an expected result for this massive structure.

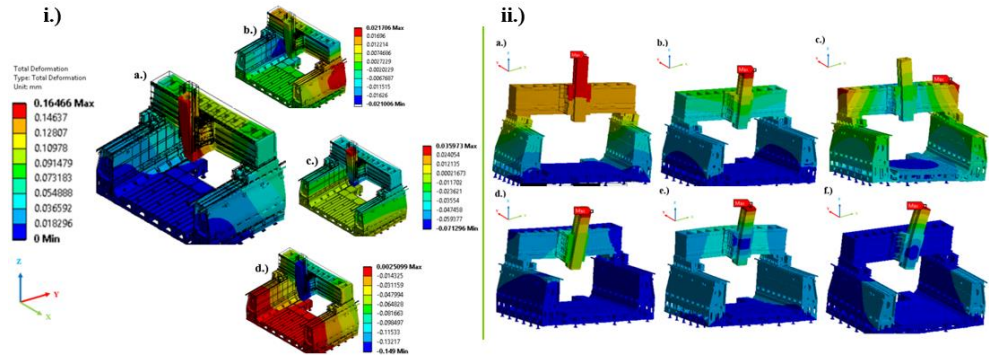


Fig.2: i.) a) The total static deformation of the CNC under gravitational force at the worst position. The directional static deformation results **b)** X-axis, **c)** Y-axis, **d)** Z-axis. **ii.)** The mode shapes of the FE analysis. **a)** 1st Mode (21.8 Hz), **b)** 2nd Mode (23.9 Hz), **c)** 3rd Mode (41.8 Hz), **d)** 4th Mode (43.8 Hz), **e)** 5th Mode (64.2 Hz), **f)** 6th Mode (69.3 Hz) shapes.

The mode shapes are indicated in Fig.2 ii. a., b., c., d., e., and f. The 1st mode shape is 21.8 Hz and makes a swinging motion along X-axis. The 2nd mode shape is 23.9 Hz, and it demonstrates a leaning motion along Y-axis. These two adjacent modes prove the casted mono-block structures behave like a single-volume structure. The 3rd mode is around 41.8 Hz and shows torsional features which are undesired for machine tool design. The 4th mode shape, which is caused by the gantry structure, is 43.8 Hz. The 5th and 6th modes are detected at 64.1 and 69.3 Hz, respectively. These mode shapes are related to the Z column and gantry structures. The natural frequencies predicted by FE is expected lower after the 4th mode due to contact parameters. The mentioned modes are related to linear guides and connection elements. However, the used contact algorithm is prone to assign oscillative (generally higher) contact stiffness values. [13].

4 Experimental Investigation

4.1 Modal Analysis

FRF measurements were conducted by impact hammer testing from 25 distinct points on the body columns. The results are presented in Table 1 comparing to those of the FE analyses. Table 1 indicates that the natural frequencies obtained by FE analyses are close to the measured data from experiments. According to Table 1, the body components of the machine tool achieves the predicted dynamic rigidity. Impact Hammer tests were also conducted on the gantry. In these measurements, FRF data were collected 20 distinct points in total. The natural frequencies and dynamic parameters obtained from the modal tests are tabulated in Table 2 comparing to those of the FE analyses. As can be seen in Table 2, the

1st Bending Mode is calculated with a lower error rate compared to the 2nd Torsional Mode by employing FEM.

The hammer tests were performed on the Z column. All measurements were repeated in the XX and YY directions, and FRF data were collected 36 points. Impact hammer test results can be seen in Table 3. The spindle has close natural frequencies to those of the machine tool structure at the X and Y directions. However, the most flexible mode of the spindle in the Y-direction is two times smaller than those in the X-direction.

Table 1: The Comparison of the results obtained from the FE analyses and impact hammer tests for the body columns (PCB 626B03 accelerometer, PCB 086C05 oversized hammer).

Modes	Natural Frequencies obtained by the FEM (Hz)	The results obtained by the Impact Hammer Test			
		Natural Frequency (Hz)	Modal Stiffness (N/m)	Damping Ratio (%)	Receptance of FRF ($\mu\text{m/N}$)
<i>1st Bending</i>	21.8	18.4	3.6×10^8	2.1	0.022
<i>1st Torsional</i>	41.8	48.8	4.8×10^9	0.9	0.011

Table 2: The Comparison of the results obtained from the FE analyses and impact hammer tests for the gantry. (PCB 626B03 accelerometer PCB 086C05 oversized hammer).

Modes	Natural Frequencies obtained by the FEM (Hz)	The results obtained by the Impact Hammer Test			
		Natural Frequency (Hz)	Modal Stiffness (N/m)	Damping Ratio (%)	Receptance of FRF ($\mu\text{m/N}$)
<i>1st Bending</i>	43.8	50.1	2.46×10^{10}	0.15	0.028
<i>1st Torsional</i>	64.2	84.6	1.33×10^{10}	1.30	0.005

Table 3: The top 3 most flexible modes of the Spindle and Z column measured by Impact Hammer tests. (PCB 353B33 accelerometer, PCB 086C05 hammer).

Modes		The results obtained by the Impact Hammer Tests			
		Natural Frequency (Hz)	Modal Stiffness (N/m)	Damping Ratio (%)	Receptance of FRF ($\mu\text{m/N}$)
<i>XX direction</i>	<i>1st Bending</i>	26.9	2.63×10^7	4.92	0.392
	<i>2nd Bending</i>	89.5	1.31×10^8	3.92	0.115
	<i>3rd Bending</i>	171.9	1.50×10^8	3.42	0.122
<i>YY direction</i>	<i>1st Bending</i>	23.7	2.44×10^7	2.81	0.823
	<i>2nd Bending</i>	106.5	8.58×10^7	4.89	0.048
	<i>3rd Bending</i>	190.9	4.98×10^8	3.31	0.037

4.2 Motion Performances of the Axes

The physical capability tests were carried out to measure the velocity, acceleration, and jerk behaviour of the X, Y, Z, A, and C axes of the machine tool. The results can be seen in Figure 3.a., 3.b. and 3.c. for linear axes. From Figure 3.a., it can be concluded that the feed rates of the linear axes can continuously go up to 1500 mm/min axial velocity, and the axes can reach 1600 mm/min axial velocity as the maximum for the feed rates higher than 1500 mm/min. This is caused by 5-mm measurement distances. A competitive regular-size CNC with a processing capacity of $\sim 500 \times 500 \times 500 \text{ mm}^3$ -volume can go up to 3500 mm/min axial velocity at a 5-mm distance. Therefore, the measured velocities in Figure 3.a. are assumed as satisfactory when the large sizes of the machine tool are considered. The acceleration and jerk behaviour of the linear axes are indicated in Figures 3.b. and 3.c., respectively. The values obtained for the rotary axes can be seen in Figures 3.d, 3.e and 3.f. As can be seen from Figure 3.e., C-axis can reach a 2000 mm/min feed rate properly, while A-axis could not catch this value.

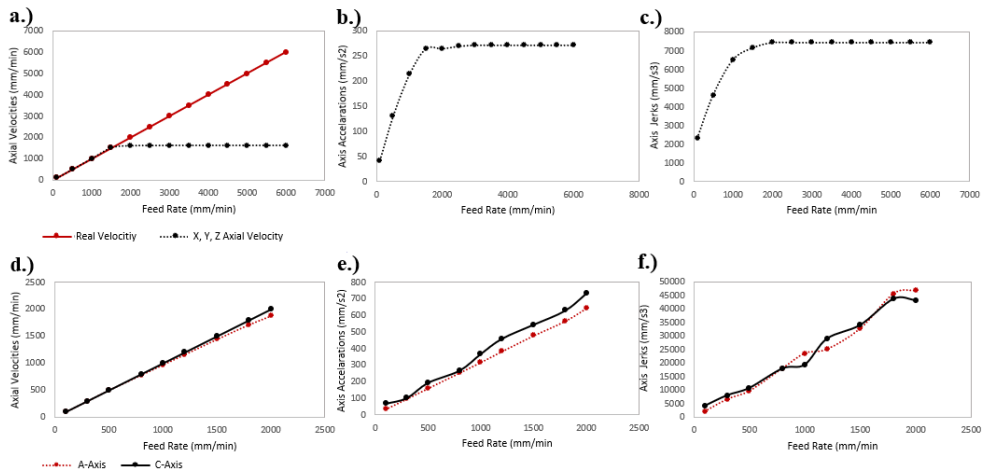


Fig.3: a.) Linear Axial Velocities, b.) Linear Axial Accelerations, c) Linear Axial Jerk profiles of X, Y, Z axes for a 5-mm translation; e.) Rotational Axial Velocities, d.) Rotational Axial Accelerations, f) Rotational Axial Jerk profiles of A and C axes for 3° rotation.

5 Conclusions

Design and analysis methods are presented for a gantry-type machine tool with large sizes. Casting-method benefited design strategies are proposed to maintain the stiffness values to build a large-size gantry-type CNC machine tool. The effectiveness of the proposed methods was evaluated by FE analyses and experiments on the manufactured prototype. The results indicate a competitive performance when the proposed casting-method benefited design strategies are employed.

References

1. S. Liu, Y. Li, Y. Liao, Z. Guo, *Str. and Mult. Opt.*, **50**, 2, 297-311. (2014).
2. X. Yang, K. Cheng, *Procedia Manufacturing*, **11**, 1454-1462, (2017).
3. P. Boral, T. Nieszporek, R. Gołębski, *MATEC Web of Conf.*, **157**, (EDP Sci, 2018).
4. M. Guillo, L. Dubourg, *Robotics and CIM*, **39**, 22-31, (2016).
5. J. Do Suh, H.S. Kim, J.M. Kim, *Comp. Sci. Tech.*, **64**, 10-11, 1523-1530, (2004).
6. E.F. Kushnir, M.R. Patel, T.M. Sheehan, *ASME-PUBS.-PVP*, **432**, 133-146, (2001).
7. G. Sproesser, Y.J. Chang, A. Pittner, M. Finkbeiner, M. Rethmeier, *Sustainable Manufacturing*, 71-84, (Springer, Cham., 2017).
8. X. Lu, X. Lin, M. Chiumenti, M. Cervera, Y. Hu, X. Ji, W. Huang, *Additive Manufacturing*, **26**, 166-179, (2019).
9. R. Schaller, *Journal of Alloys and Compounds*, **355**, 1-2, 131-135, (2003).
10. Y. Altintas, C. Brecher, M. Weck, S. Witt, *CIRP annals*, **54**, 2, 115-138, (2005).
11. L. Zhang, L. Ma, D. Wu, Y. Zhou, *The Int. J. of Adv. Manuf. Tech.*, **104**, 1-4, 245-260, (2019).
12. W.U. Tao, L.G. CAI, *DEStech Tr. on Eng. and Tech. Res.*, (amee), (2018).
13. E. Yuksel, A.S. Erturk, E. Budak, *E. J. of Manuf. Sci. and Eng.*, **142**, 8, (2020).
14. T. Murakami, T. Inoue, H. Shimura, M. Nakano, S. Sasaki, *Mat.Sci.and Eng, A*, **432**, 1-2, 113-119. (2006).